Probabilistic fracture analysis for LMFBR piping integrity

J.Matsumoto & M.Idesawa
Nuclear Power R&D Center, Tokyo Electric Power Co., Inc., Japan
D.O.Harris
Failure Analysis Associates, Palo Alto, Calif., USA
S.A.Eide
Energy Incorporated, Idaho Falls, USA
T.Oyama
Nippon Energy Incorporated, Tokyo, Japan
G.Yagawa
Department of Nuclear Engineering, University of Tokyo, Japan

1 INTRODUCTION

In a commercial LMFBR it is necessary to design systems rationally, in accordance with the safety goals, while keeping construction costs to a minimum. In the case of sodium leakage from the primary or secondary heat transfer systems, one of the most important design base accidents, a large leak size is assumed at the prototype LMFBR stage, resulting in an excessively large sodium leak safety system. For example, both MONJU and CRBRP estimate the maximum leak size to be 0.25DT (D:diameter of piping, T:thickness of piping). When the probabilistic fracture mechanics code is applied to LMFBR piping, the probability of small and large leaks and a DEGB (Double Ended Guillotine Break) can be estimated as a function of plant life time. Valuable data regarding the maximum sodium leak size may be obtained in this way.

One problem with the probabilistic fracture analysis of LMFBR piping is the reliability of the results. Progress can be made by refining the models employed and by improving the reliability of the data. Therefore it is important to give priority to these aspects, taking into consideration the fracture mechanics models which yield the most effective information.

2 METHODOLOGY

This section outlines the modification and additions which were made to the LWR PRAISE-B probabilistic fracture mechanics code (Ref. 1, 2, 3) to make it applicable to LMFBR piping. Basically, this code, assumes that failure results from the growth of crack-like defects introduced during fabrication. The major modifications made to the PRAISE-B fracture mechanics model are as follows:

(1) initial crack distribution, (2) crack detection probability, (3) crack growth characteristics, (4) sodium leak flow rate, (5) failure criteria
Each of these is discussed below.

2.1 Initial Crack Distribution

In this fracture mechanics model, the major difference between LWRs and LMFBRs is the wall thickness of the piping. The initial crack distribution is sub-divided into crack depth distribution, aspect ratio and crack existence probability. The way these are modelled in PRAISE-B is also applicable to LMFBR piping.

Most probabilistic fracture mechanics codes employ the so-called Marshall distribution for the conditional marginal distribution of crack depth. The Marshall distribution is exponential, and is normalized to the pipe wall thickness, which results in the following density function:

$$p(a) = \frac{e^{-a/\mu}}{\mu\ (1 - e^{-h/\mu})}$$

where μ= mean crack depth, a=crack depth, h=wall thickness.
Also, the PRAISE-B aspect ratio distribution may be applied to LMFBR piping, because of the lack of the information about the actual LMFBR crack aspect ratio distribution

$$p_{\beta}(\beta) = \frac{C_{\beta}}{\lambda\,\beta\,\sqrt{2\pi}}\, e^{-\left(\ln \frac{\beta}{\beta_m}\right)^2/(2\lambda^2)}$$

where β=aspect ratio (equals b/a, b=half surface length of a semi-elliptical surface crack), β_m, λ=parameters for the marginal distribution of the initial crack aspect ratio, C_{β}=constant for the distribution of initial crack aspect ratio

Finally, the crack existence probability is assumed to be 1.0×10^{-4} /inch^3 (6.1×10^{-6}/cm^3) in accordance with discussions in Ref. 1.

2.2 Crack Detection Probabilities (Ref. 4)

PRAISE-FBR uses the following expression, which is the same as that used in PRAISE-B, for the nondetection probabilities of surface flaws in austenitic stainless steel weldments using ultrasonic inspection:

$$P_{ND}(A) = \varepsilon + 0.5\ (1 - \varepsilon)\ \mathrm{erfc}\ \left(\gamma\ \ln\left(\frac{A}{A^*}\right)\right)$$

where ε=minimum nondetection probability, γ=parameter in the expression for P_{ND}, A=area of crack A*=crack area having a 50% chance of being found during inspection

2.3 Crack growth characteristics

(1) Fatigue
As the temperature is in the creep range, a modified Paris Crack growth relation is used, as given below:

$$\frac{da}{dN} = C_1\, \Delta K_{eff}^{\bar{m}}$$

where $\Delta K_{eff}=\Delta K/(1-R)^{1/2}$. The scatter in the value of da/dN for a given ΔK_{eff} is accounted for by considering C_1 to be a random variable. As reported in Ref. 5, m can be taken to be three for the material considered, and the distribution of C_1 can be described as a lognormal function, with a median value, C_{50} of 1.1×10^{-9}. The probability density function of C_1 is

$$p(C_1) = \frac{1}{\sqrt{2\pi}\ \eta C_1} e^{-\frac{1}{2\eta^2}\left(\ln \frac{C_1}{C_{50}}\right)}$$

where $\eta=0.410$

(2) Creep

The stresses near a crack tip in a body undergoing steady-state creep are controlled by the parameter, C*. The uniaxial stress-strain rate relation is of the form

$$\dot{\varepsilon} = A_1 \sigma^6$$

where $A_1=5.58 \times 10^{-20}$ for stress in MPa and strain rate in hr^{-1}. The similarity between this relation and the power law hardening plasticity allow C* to be evaluated from corresponding J-integral solutions. Under steady-state, the creep crack growth rates can be correlated to the value of C*, in the form

$$\frac{da}{dt} = C_3 C^{*m}$$

Using Saxena data (Ref. 6), m and C_3 become 0.04 and 0.63. C* solutions are interpolated for Ri/h=20 (Ri=inside radius, see Table 2) from Ref. 8.

(3) Creep/Fatigue interactions

The crack growth considering creep/fatigue interaction is given by

$$\frac{da}{dN} = C_1 \Delta K^n + C_2 \Delta K^{2m} t_h^{1-m} + C_3 C^{*m} t_h$$

where th = hold time

The same equation can be applied to the b-direction. The 1st, 2nd and 3rd terms mean the fatigue effect, the creep/fatigue effect and the creep effect. C_1 and C_3 are as given in the above equations. This treatment is applicable to very long duration transients. A curve fit to the experimental data of Ref. 5 provides a value for C_2 of 1.0×10^{-6}. The above equation agrees well with the experimental data given in Ref. 5.

2.4 Sodium leak flow rate

The sodium leak flow rate is given below assuming that the crack is idealized as a long, thin, rectangular region and that the steady-state momentum equation relating the pressure drop across the pipe wall to the friction force acting on the liquid sodium is satisfied.

$$W = \frac{\rho_\ell}{8\mu_\ell h} \delta_c^3 (2b) \Delta P$$

where ρ_ℓ=liquid sodium density, μ_ℓ=sodium viscosity, δc=opening

displacement, ΔP=pressure drop across the pipe wall

2.5 Failure criteria

PRAISE-FBR adds a tearing instability failure criterion. The tearing instability criterion is stated such that failure will occur if

$$T_{applied} > T_{MAT} \quad (T = \frac{E}{\sigma_{flo}} (\frac{dJ}{da}) \ , \ \sigma_{flo} = \text{flow stress})$$

and

$$J \text{ applied} > J_{IC}$$

The J-integral solutions for complete circumferential and through-wall cracks are obtained from information in Ref. 8.

3. ANALYSIS

PRAISE-FBR runs were performed on sample problems for a number of different cases. Table 1 shows the parameters used for each case: Table 2 shows the conditions used in the calculations:

3.1 Basic Analysis

(1) Crack extension from a given crack size
PRAISE-FBR can also calculate crack growth deterministically. An initial crack size of a=0.125 inch (0.3175 cm) and b=0.75 inch (1.905 cm), was set, and then the crack extension was calculated. The results are shown in Table 3.
(2) Leak probabilities
Leak probabilities were calculated under the same conditions given above except that crack size distribution and nondetection probability, were considered. The crack size distribution and nondetection probability, were set to make the probability of a crack depth exceeding 0.125 inch (0.3175 cm) less than one percent. The results are shown in Table 4, this corresponds to case 1 or Table 1.

3.2 Sensitivity Analysis

Sensitivity analysis was performed for the cases given in Table 1. The results are shown in figures 1 - 4.

4. CONCLUSIONS

4.1 Basic Analysis

Creep effect dominates crack growth. Fatigue crack growth is small. This is a result of the low stress and small number of cycles involved, which are too low for significant fatigue crack growth.

4.2 Sensitivity Analysis

(1) The calculated leak probability is sensitive to the mean crack

depth used (see Figure 1). This is because the stress intensity factor is a strong function of crack depth.
(2) The calculated leak probability is not sensitive to the aspect ratio of the cracks (see Figure 2).
(3) Nondetection probability is a sensitive factor (see Figure 3). This is because the probability of nondetection of cracks changes the distribution of crack depth.
(4) The data used in this report was measured in an air-environment at 1000°F (537.8°C). It is reasonable to expect that a sodium-environment will reduce crack growth due to both creep and fatigue effects. Another calculation using Nikbin data was performed, and the results are shown in Figure 4.
(5) A3 gpm (561000 gr/hr) sodium leak is taken to be the detectable leak rate, and it is assumed that this will result in a plant shut down. The cumulative leak probability is 7.76×10^{-7}. Even if the leakage would be happened, the leakage should be detected when the leakage becomes 3 gpm (561000 gr/hr), whose corresponding break area is about 0.04 cm^2, and the probability of 3 gpm (561000 gr/hr) is 1.64×10^{-8}. Therefore, when it becomes necessary to assume a break area for a certain conservative requirements, a smaller break area than 0.25DT may be assumed.
(6) The flow stress, critical depth of part-through crack, and critical half surface length of through-wall crack corresponding due to J_{IC} and T_{MAT} criteria are 37.23 ksi (256.7 MPa), 0.49 inch (1.245 cm) and 6.232 inch (15.83 cm) respectively, and in this case, J_{IC} and T_{MAT} criteria are more limiting than the critical net section. When critical net section is adopted as the failure criteria, the crack growth stops after the leak rate exceeds the detectable leak rate, and does not develop into a DEGB. However, in the case of the J_{IC} and T_{MAT} criteria, there is a small probability of 8.16×10^{-13} (case 9 of Table 1), that a DEGB may occur.

On the other hand, if the leak is not detected, the crack will continue to grow into a through-wall defect and may eventually lead to a DEGB, given sufficient time, even in the cases when critical net section failure criteria are used. If a calculation is made, neglecting leak detection, the DEGB probability is 2.66×10^{-14}, and the critical crack size, bc, is 31 inch (79.43 cm). In reality, however, leakage can be detected when b is about 2 inches which corresponds to the detectable limit of 3 gpm (561000 gr/hr). Therefore, the probability of a DEGB will be less than this value.

4.3 Recommendations for future work

The models reported herein provide the first step in the development of a probabilistic fracture mechanics code for a LMFBR.

For the further improved analysis of LMFBR piping integrity, it is recommended that numerous crack growth experiments should be carried out under high temperature conditions and in sodium environments to provide better growth characteristic data. Also non destructive inspection techniques should be developed and the initial crack distribution should be better defined as the leak and DEGB probabilities are very sensitive to these factors.

REFERENCES

1. Harris, D.O., E.Y. Lim & D.D. Dedhia, 1981, Probability of pipe Fracture in the Primary Coolant Loop of a PWR Plant, Vol. 5: Probabilistic Fracture Mechanics Analysis, U.S. Nuclear Regulatory Commission, NUREG/CR-2189, Vol. 5, Washington, D.C.
2. Lim, E.Y., 1981, Probability of Pipe Fracture in the Primary Coolant Loop of a PWR Plant, Vol. 9: PRAISE Computer Code User's Manual, U.S. Nuclear Regulatory Commission, NUREG/CR-2189, Vol. 9, Washington, D.C.
3. Harris, D.O., E.Y. Lim, D.D. Dedhia, H.H. Woo & C.K. Chow, 1982, Fracture Mechanics Models Developed for Piping Reliability Assessment in Light Water Reactors, U.S. Nuclear Regulatory Commission, NUREG/CR-2301, Washington, D.C.
4. Harris, D.O., 1985, Probabilistic Fracture mechanics, Pressure Vessel and Piping Technology, 1985-A Decade of Progress, ASME, PP.771-791
5. James, L.A. & D.P. Jones, 1985, Fatigue Crack Growth Correlations for Austenitic Stainless Steal in Air, Prediction Capabilities in Environmentally Assisted Cracking, PVP Vol. 99, PP.363-414
6. Saxena, A., 1980, Evaluation of C* for the Characterization of Creep-Crack-Growth Behavior in 304 Stainless Steal, Fracture Mechanics: Twelfth Conference, ASTM STP 700, Philadelphia, PP.131-151
7. Nikbin, K.M., D.J. Smith & G.A. Webster, 1984, Prediction of Creep Crack Growth from Uniaxial Creep Data, Proceedings of the Royal Society of London, Vol. A396, PP.183-197
8. Kumar, V., M.D. German & C.F. Shih, 1981, An Engineering Approach for Elastic-Plastic Fracture Analysis, Electric Power Research Institute, EPRI NP-1931
9. Westinghouse Electric Corporation, 1977, Integrity of Primary and Intermediate Heat Transport System Piping in Containment, Vol. 1 and 2 (Clinch River Breeder Reactor Plant), WARD-D-0185

Table 1 Summary of parameters used in calculations[1),2)]

Parameter	Case	1	2	3	4	5	6	7	8	9
Crack size distribution	μ=0.625 cm		o							
	μ=0.170 cm	o			o	o	o	o	o	o
	μ=0.094 cm			o						
Aspect ratio	20% (β>5)				o					
	1% (β>5)	o	o	o			o	o	o	o
	0.01% (β>5)					o				
Nondetection probability (Pre-service inspection only)	ε=0.005 a*=0.635 cm						o			
	ε=0.005 a*=0.127 cm	o	o	o	o	o			o	o
	ε=0.001 a*=0.127 cm							o		
Failure criteria	Critical net section	o	o	o	o	o	o	o	o	
	JIC-TMAT									o
Creep characteristics	Saxena's data	o	o	o	o	o	o	o		o
	Nikbin's data (Ref. 7)								o	

1) Case 1 is the base case.
2) "o" indicates the paramter used in each case.

Table 2 Summary of calculation conditions

Pipe geometry (same as the 24 inch hot leg piping of Ref. 9)	Pipe radiuas 11.5 inch (29.21 cm) Wall thickness 0.5 inch (1.27 cm)
Material	SUS 304
Stresses	Heat up stress 5.0 ksi (34.5 MPa) Shutdown stress 0.0 ksi (0.0 MPa)
Temperature	537.8 °C
Pressure	0.168 ksi (1.16 MPa)
Plant lifetime	30 years
The number of plant shutdowns in the plant lifetime	150 cycles (5 events/year)

Table 3 Final crack size of an initial 0.125 inch (1.905 cm) crack

Effect of Fatigue alone	Effect of Fatigue and Creep without interactions	Effect of Fatigue and Creep with Interactions
0.125004 inch (0.31751 cm)	0.1505 inch (0.38227 cm)	0.1627 inch (0.41326 cm)

Table 4 Cumulative Leak Probabilities

Effect of Fatigue alone	Effect of Fatigue and Creep without interactions	Effect of Fatigue and Creep with Interactions	
		Small leak (< 3 gpm)	Big leak (≧ 3 gpm)
6.66×10^{-10}	7.36×10^{-7}	7.76×10^{-7}	1.64×10^{-8}

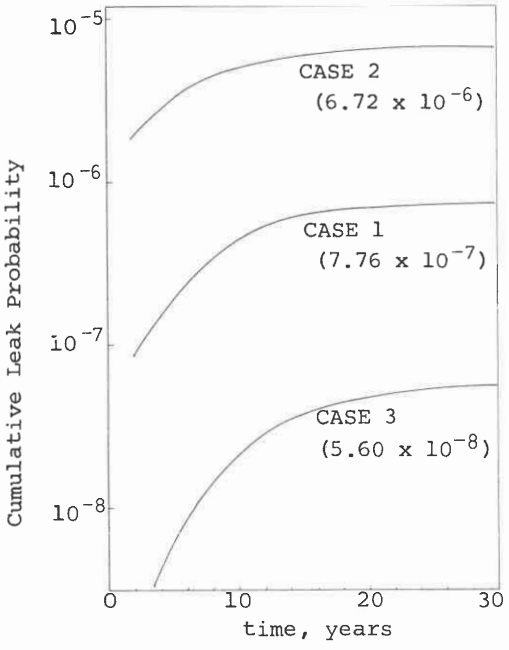

Figure 1

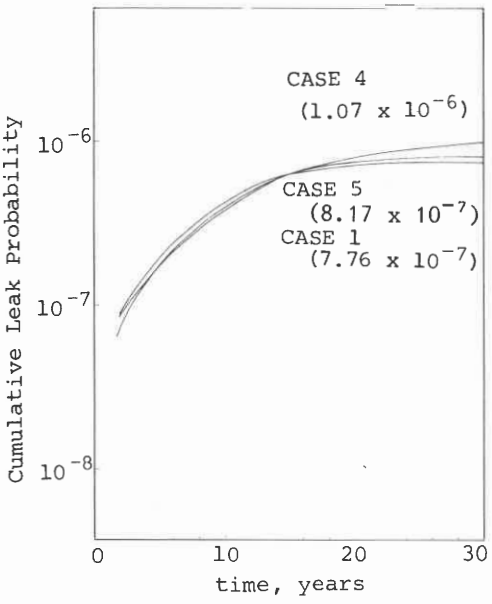

Figure 2

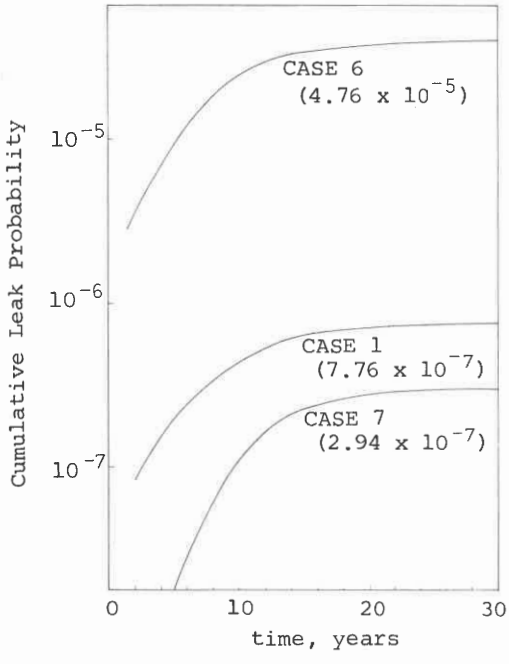

Figure 3

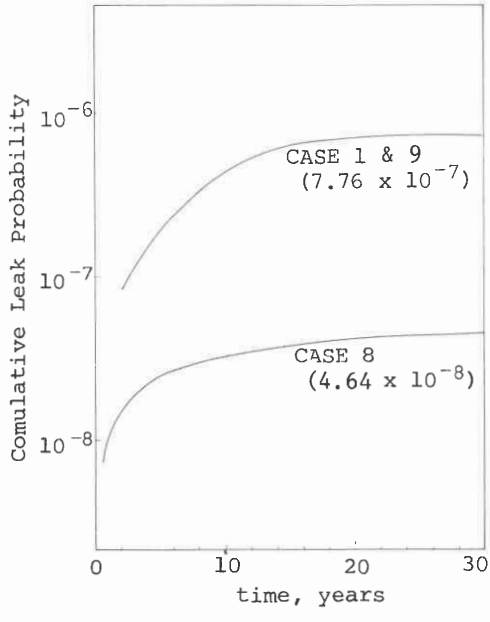

Figure 4

Cumulative leak probabilities as a function of time for base conditions and for each parameter.
Figure 1, 2, 3 and 4 are for various mean crack depth, various aspect ratios, various nondetection probabilities and the NIKBIN's data, respectively.